Electronic Supplementary Information

Integration of peptide-DNA conjugate with multiple cyclic signal amplification for ultrasensitive detection of cathepsin B activity

Zi-yue Wang‡, Cheng-peng Zhang‡, Chun-yang Zhang*

College of Chemistry, Chemical Engineering and Materials Science, Collaborative Innovation Center of Functionalized Probes for Chemical Imaging in Universities of Shandong, Key Laboratory of Molecular and Nano Probes, Ministry of Education, Shandong Provincial Key Laboratory of Clean Production of Fine Chemicals, Shandong Normal University, Jinan 250014, P.R. China

* Corresponding author. Tel.: +86 0531-86182538; Fax: +86 0531-82615258; E-mail: cyzhang@sdnu.edu.cn.

‡ These authors contributed equally.

EXPERIMENTAL SECTION

Chemicals and materials. All oligonucleotides (Table S1) and diethylpyrocarbonate (DEPC)-treated water were purchased by Takara Biotechnology Co. Ltd. (Dalian, China), and the peptide C_{term}-Biotin-KGFRLC-N_{term} was synthesized by Chinese Peptide Company (Hangzhou, Zhejiang, China). The connection of N terminal of peptide with 5' terminal of DNA for the formation of a peptide-DNA conjugate was achieved by Takara Biotechnology Co. Ltd. (Dalian, China). Cathepsin B, Cathepsin L, Cathepsin S, antipain and leupeptin were purchased from Sigma-Aldrich Company (St. Louis, MO, USA). Cathepsin D was bought from R&D System (Minneapolis, MN, U.S.A.). Streptaridin magnetic beads, Bst. DNA polymerase (large fragment),

10× ThermoPol reaction buffer (200 mM Tris-HCl, 100 mM ammonium sulfate ($(NH_4)_2SO_4$), 100 mM KCl, 20 mM magnesium sulfate ($MgSO_4$), 1% Triton X-100, pH 8.8), Nt.BstNBI, 10× NEBuffer 3.1 (1000 mM NaCl, 500 mM Tris-HCl, 100 mM $MgCl_2$, 1 mg/mL bovine serum albumin (BSA), pH 7.9), RNase H, 10× RNase H reaction buffer (500 mM Tris-HCl, 750 mM KCl, 30 mM $MgCl_2$, 100 mM DTT, pH 8.3), RNase inhibitor, deoxyribonucleoside 5'-triphosphate mixture (dNTPs) were obtained from New England Biolabs (Beverly, MA, U.S.A.). SYBR Gold was purchased from Life Technologies (Carlsbad, CA, U.S.A.). Human cervical carcinoma cell line (HeLa cells) and human embryonic kidney cell line (HEK-293 cells) were obtained from Cell Bank, Shanghai Institutes for Biological Sciences, Chinese Academy of Sciences (Shanghai, China). Other analytical grade chemicals were used without further purification. Ultrapure water used in this research was obtained from a Millipore filtration system, and DEPC-treated water was used for the experiments involving peptides and RNA. In addition, cathepsin B and the cell lysate need to be pre-activated for 10 min at 37 °C in 5 mM dithiothreitol (DTT) and 25 mM 2-(4-morpholino) ethane sulfonic acid (MES) buffer (pH 5.0) to obtain the full activity before the enzymic hydrolysis reaction.

Table S1. Sequences of the oligonucleotides [α]

note	sequences (5'-3')
template 1	CGT GAA TAA CTC TAC TAT CAA CAG AC TCC ACA AAT TCG ACC AAC AGA CTC ACT ACG ACC GGG AC-P
template 2	AAC AGA CTC ACT ACG ACC GGG ACA ACA GAC TCC ACA AAT TCG ACC AAC AGA CTC CGT GAA TAA CTC TAC TAT C-P
peptide-DNA conjugate	C_{term}-Biotin-KGFRLC-N_{term}-GTC CCG GTC GTA GTG AGT CT
signal probe	FAM-rArUrArArCrUrCrUrArCrUrArUrC-BHQ1

[α] In template 1 and template 2, the "P" indicates the phosphate group (PO_4) modification at the 3′ end, and the underlined regions represent the recognition site of Nt.BstNBI. The lower-case letter of r in the signal probe symbolizes the ribonucleotide.

Cell Culture and the preparation of cell extracts. HeLa cells and HEK-293 cells were maintained in Dulbecco's modified Eagle's medium (DMEM; Gibco, U.S.A.) supplemented with 10% fetal bovine serum (FBS, Gibco, U.S.A.) and 1% penicillin-streptomycin (Gibco, U.S.A.) in a humidified atmosphere containing 5% CO_2 at 37 °C. Cells were collected with trypsinization in the exponential phase of growth. The medium was removed and the cells were washed twice with cold 1× PBS (pH 7.4, Gibco, U.S.A.), and centrifuged at 1000 rpm for 5 min. The 100 μL of lysis buffer (10 mM Tris-HCl, pH 8.0, 150 mM NaCl, 1% NP-40, 0.25 mM sodium deoxycholate, 1.0% glycerol, and 0.1 mM 4-(2-aminoethyl) benzenesulfonyl fluoride hydrochloride) was used to suspend the cells, and then the mixture was incubated on ice for 30 min, followed by centrifugation at 12000 g for 20 min at 4 °C. The supernatant was carefully transferred to a fresh

tube and the pH was carefully adjusted to 5.5.

Integration of peptide-DNA conjugate with multiple cyclic signal amplification. This assay involved three steps. First, the peptide-DNA conjugates were diluted with DEPC-treated water to prepare the stock solutions. The 20 μL of streptavidin-coated magnetic bead solution (4 mg/mL) was transferred into a 200-μL centrifuge vial and washed twice with 1× B&W buffer (5 mM Tris-HCl, pH 7.5, 0.5 mM EDTA, 1 M NaCl), and the magnetic bead was resuspended in 20 μL of 2× B&W buffer (10 mM Tris-HCl, pH 7.5, 1 mM EDTA, 2 M NaCl). Subsequently, 30 μL of 1 μM biotinylated peptide-DNA conjugates was added into the solution and incubated for 15 min at room temperature with rotation. The mixture was then washed three times using 50 μL of 1× B&W buffer to remove the uncoupled peptide-DNA conjugates, and the remaining peptide-DNA-magnetic bead conjugates were dispersed in 20 μL of DEPC-treated water. Second, 5 μL of peptide-DNA-magnetic bead conjugates was added into the cathepsin B excision reaction system (20 μL) containing 1× cathepsin B reaction buffer and the activated cathepsin B at different concentrations, and the solution was incubated at 37 °C for 1 h for the peptide-DNA conjugate cleavage. In this process, cathepsin B recognized and cleaved the peptide part in the peptide-DNA conjugate, leading to the dissociation of DNA part from the magnetic bead. After magnetic separation, the supernatant containing the released DNA part was obtained for later use. Third, 2 μL of supernatant containing the released DNA part was added into the cycle signal amplification reaction system (20 μL) containing 25 nM template 1, 25 nM template 2, 500 μM dNTPs, 2.4 U of Bst.DNA polymerase, 10 U of Nt.BstNBI, 700 nM signal probe, 1 U of RNase H, 20 U of RNase inhibitor, 2 μL of 10× NEBuffer 3.1, 2 μL of 10× ThermoPol buffer, and 2 μL of 10× RNase H buffer, and the mixture was incubated at 37 °C for 50 min for enzyme-assisted

cascade signal amplification. In this process, both multiple strand displacement reactions and ribonuclease H-medicated cycle digestion of signal probes proceeded. The multiple strand displacement reactions induced the cycles of extension, nicking, and displacement to produce abundant trigger Z, and the released trigger Z can bind with the signal probe, initiating the ribonuclease H-medicated cycle digestion of signal probes and resulting in an enhanced FAM fluorescence.

Real-time fluorescence measurement and gel electrophoresis. We used real-time fluorescence measurement to monitor multiple strand displacement reactions process. As the amplification reaction proceeded, more and more strands were produced, resulting in an enhanced fluorescence signal. This process was monitored at the intervals of 30 s with a BIO-RAD CFX connect TM Real-Time System (California, U.S.A.), and 1× SYBR gold was used as the fluorescent indicator, The 14% nondenaturating polyacrylamide gel electrophoresis (PAGE) was performed to analyze the reaction products in 1× TBE buffer (9 mM Tris-HCl, 9 mM boric acid, 0.2 mM EDTA, pH 7.9) at a 110 V constant voltage for 60 min at room temperature in the dark, and 1× SYBR gold was used as the fluorescent indicator.

Inhibition assay. Various-concentration leupeptin and antipain were incubated with cathepsin B in the cathepsin B excision reaction system, respectively. Then 2 μL of reaction products were added into the cycle signal amplification reaction system. The relative activity of cathepsin B was calculated according to eq. 1:

$$\text{Relative activity (\%)} = \frac{F_i - F_0}{F_t - F_0} \times 100\% \qquad (1)$$

Where F_t represents the fluorescence intensity in the presence of cathepsin B, F_i represents the fluorescence intensity in the presence of cathepsin B and different-concentration inhibitors, and F_0

represents the fluorescence intensity in the absence of cathepsin B and inhibitor.

Measurement of fluorescence emission spectra. The 20 μL of reaction products was diluted to 60 μL with ultrapure water. The fluorescence signals were measured by using a Hitachi F-7000 fluorescence spectrophotometer (Tokyo, Japan) with an excitation wavelength of 490 nm, and the emission spectra was scanned from 500 to 650 nm, and the fluorescence intensity at the emission wavelength of 520 nm was used for data analysis.

SUPPLEMENTARY RESULTS

1. Optimization of experimental conditions. The fluorescence signal is significantly influenced by the amplification time, the amounts of polymerase, restriction enzyme, RNase H, and the concentration of signal probe. To achieve the best performance, we optimized these parameters.

1.1. Optimization of the amounts of DNA polymerase and Nt.BstNBI. The DNA polymerase and restriction enzyme are crucial to the signal amplification efficiency.[1, 2] We investigated the amounts of DNA polymerase and Nt.BstNBI upon the fluorescence signal. As shown in Fig. S1A, the $F - F_0$ value enhances with the increasing amount of DNA polymerase from 1.2 to 2.4 U (F is the fluorescence intensity in the presence of cathepsin B, and F_0 is the fluorescence intensity in the absence of cathepsin B), and reaches the maximum value at 2.4 U. Thus, 2.4 U of DNA polymerase is used in the subsequent experiments. We further investigated the influence of restriction enzyme Nt.BstNBI upon the fluorescence signal. As shown in Figure S1B, the $F - F_0$ value enhances with the increasing amount of restriction enzyme Nt.BstNBI from 4 to 10 U, and reaches the highest value at 10 U. Thus, 10 U of restriction enzyme Nt.BstNBI is used in the subsequent experiments.

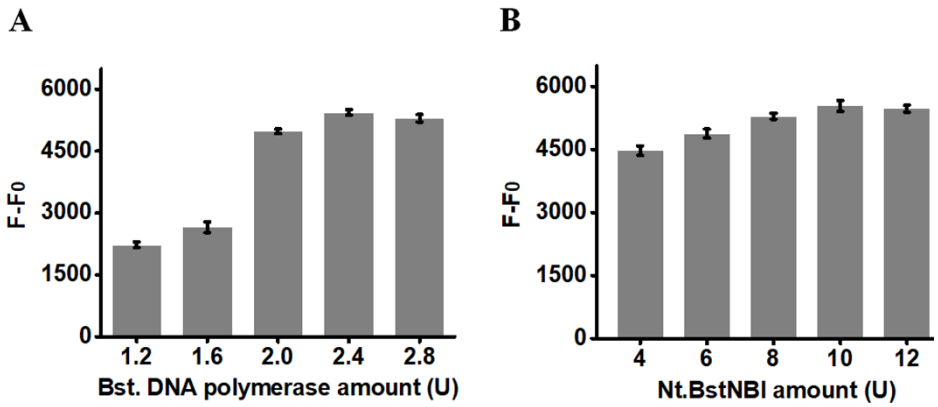

Fig. S1 (A) Variance of the $F - F_0$ value with the amount of Bst. DNA polymerase. (B) Variance of the $F - F_0$ value with the amount of Nt.BstNBI. F is the fluorescence intensity when cathepsin B is present, and F_0 is the fluorescence intensity when cathepsin B is absent. The cathepsin B concentration is 1×10^{-7} g/mL. The fluorescence intensities are obtained at 50 min. Error bars show the standard deviation of three independent experiments.

1.2. Optimization of the time of cycle signal amplification. We further investigated the time of cycle signal amplification upon the fluorescence signal. As shown in Fig. S2, the $F - F_0$ value increases with the reaction time from 20 to 50 min, and reaches a plateau beyond 50 min. Thus, the amplification reaction time of 50 min is used in the subsequent experiments.

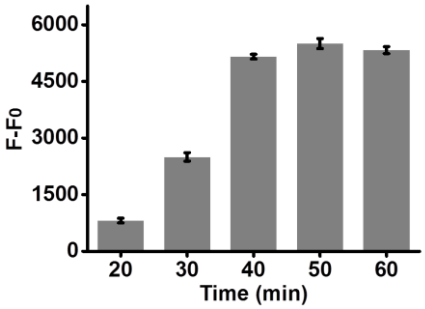

Fig. S2 Variance of the $F - F_0$ value with the amplification time. F is the fluorescence intensity when cathepsin B is present, and F_0 is the fluorescence intensity when cathepsin B is absent. The cathepsin B concentration is 1×10^{-7} g/mL. The fluorescence intensities are obtained at 50 min.

Error bars show the standard deviation of three independent experiments.

1.3. Optimization of the concentration of signal probe and the amount of RNase H. We investigated the concentration of signal probe and the amount of RNase H upon the fluorescence signal. The high concentration of signal probe will result in the high hybridization efficiency and the high fluorescence enhancement, but it is accompanied by the high background signal. Thus, the concentration of signal probe should be optimized. As shown in Fig. S3A, the $F - F_0$ value improves with the increasing concentration of signal probe from 100 to 700 nM, and reaches the maximum value at 700 nM. Thus, 700 nM signal probe is used in the subsequent experiments. The amount of RNase H may affect the digestion performance of signal probes, and it should be optimized. As shown in Fig. S3B, the $F - F_0$ value enhances with the increasing amount of RNase H, and reaches a plateau at the amount of 1 U. Thus, 1 U of RNase H is used in the subsequent experiments.

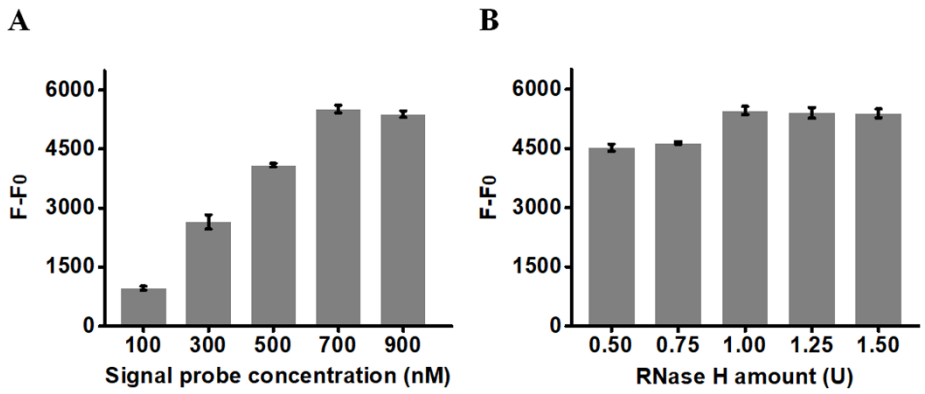

Fig. S3 (A) Variance of the $F - F_0$ value with the concentration of signal probe. (B) Variance of the $F - F_0$ value with the amount of RNase H. F is the fluorescence intensity when cathepsin B is present, and F_0 is the fluorescence intensity when cathepsin B is absent. The cathepsin B concentration is 1×10^{-7} g/mL. The fluorescence intensities are obtained at 50 min. Error bars

show the standard deviation of three independent experiments.

2. Detection specificity. To evaluate the detection specificity of the proposed method, we used cathepsin S, cathepsin L and cathepsin D as the nonspecific proteins. As shown in Fig. S4, a remarkable fluorescence signal at the emission wavelength of 520 nm is observed in the presence of cathepsin B (red column, Fig. S4), but no enhanced fluorescence signal is detected in the presence of cathepsin S (green column, Fig. S4), cathepsin L (purple column, Fig. S4), and cathepsin D (blue column, Fig. S4), suggesting the good selectivity of the proposed assay towards cathepsin B.

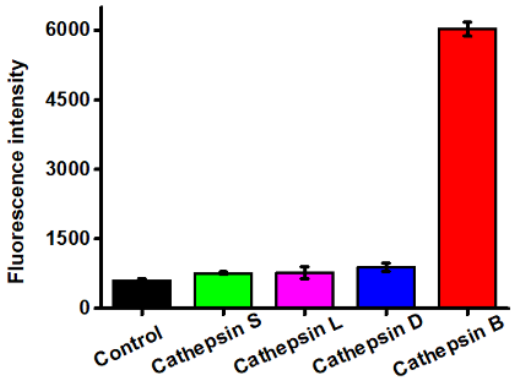

Fig. S4. Measurement of fluorescence intensity in response to the reaction buffer (control, black column), 1×10^{-7} g/mL cathepsin S (green column), 1×10^{-7} g/mL cathepsin L (purple column), 1×10^{-7} g/mL cathepsin D (blue column), and 1×10^{-7} g/mL cathepsin B (red column). Error bars show the standard deviations of three independent experiments.

3. Inhibition assays. To demonstrate the feasibility of the proposed method for screening cathepsin B inhibitors, we used leupeptin and antipain as the model inhibitors. As shown in Figure S5, both leupeptin (orange column, Fig. S5) and antipain (green column, Fig. S5) can induce the

decrease of fluorescence intensity, and the relative activity of cathepsin B decreases with the increasing concentration of leupeptin (Fig. S6B) and antipain (Fig. S6D).

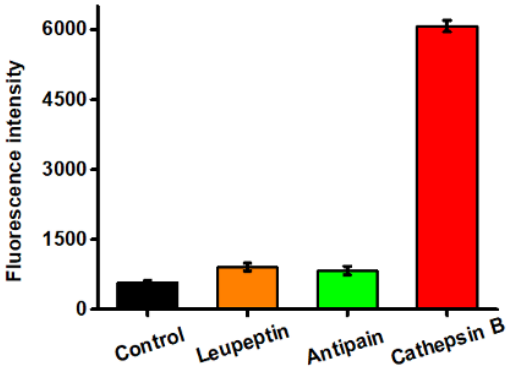

Fig. S5 Inhibition effect of 2 μM leupeptin and 2 μM antipain upon the activity of cathepsin B. The concentration of cathepsin B is 1×10^{-7} g/mL. Error bars show the standard deviations of three independent experiments.

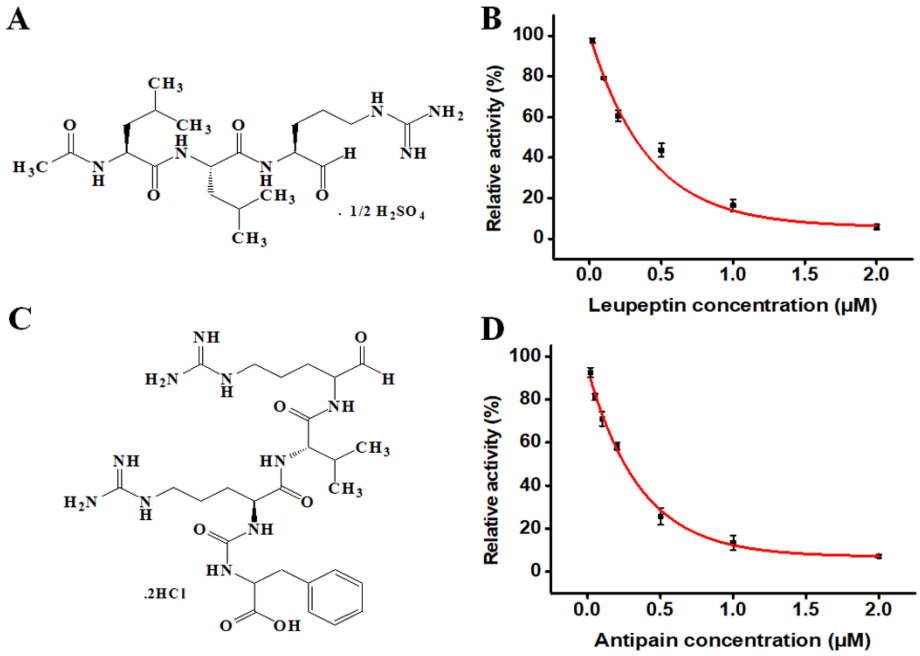

Fig. S6 (A) Structure of leupeptin. (B) Leupeptin induces concentration-dependent decrease of the relative activity of cathepsin B. (C) Structure of antipain. (D) Antipain induces concentration-dependent decrease of the relative activity of cathepsin B. The concentration of

cathepsin B is 1 × 10^{-7} g/mL. Error bars show the standard deviations of three independent experiments.

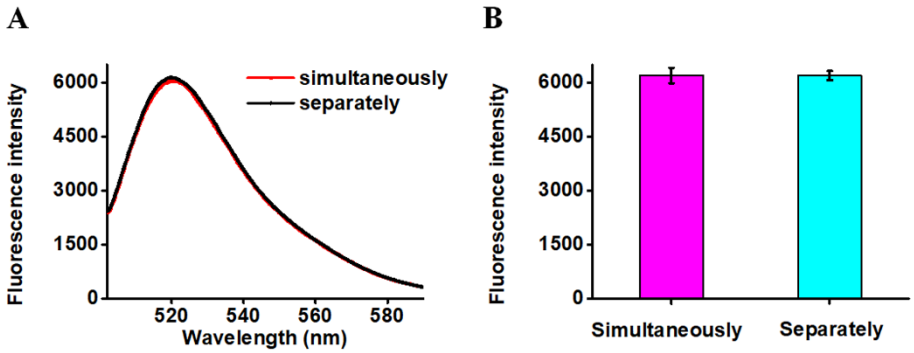

Fig. S7 (A) Measurement of fluorescence emission spectra in response to Bst.DNA polymerase + Nt.BstNBI + RNase H added simultaneously (red line) and Bst.DNA polymerase + Nt.BstNBI and RNase H added separately (black line), respectively. (B) Measurement of fluorescence intensity in response to Bst.DNA polymerase + Nt.BstNBI + RNase H added simultaneously (purple column) and Bst.DNA polymerase + Nt.BstNBI and RNase H added separately (wathet colomn), respectively. No significant difference in the measured fluorescence intensity at the emission wavelength of 520 nm is observed between them.

Table S2. Comparison of the proposed method with the reported methods for cathepsin B assay

strategy	assay time*	detection limit	cell analysis	reference
fluorescent assay based on peptide-DNA conjugate and multiple cyclic signal amplification	~2.5 h	8.1×10^{-12} g/ml, 1 cell	yes	this work
colorimetric assay based on gold nanoparticles	overnight	2.2×10^{-7} g/ml	no	3
fluorescence imaging based on multifunctional metal−organic framework nanoprobe	~50 h	1 cell	yes	4
electrochemical detection based on carbon nanofiber nanoelectrode arrays	~36 h	2.4×10^{-6} g/ml	yes	5
confocal fluorescence imaging based on cathepsin B-activatable nanoprobe	~25 h	1 cell	yes	6
fluorescence imaging based on fluorescent dendrimers	~15 h	1 cell	yes	7
electrochemical activity assay based on carbon nanofiber nanoelectrode arrays	~3.5 h	1.4×10^{-8} g/ml	no	8

* Assay time includes the preparation time.

References

1. H. Q. Wang, W. Y. Liu, Z. Wu, L. J. Tang, X. M. Xu, R. Q. Yu and J. H. Jiang, *Anal. Chem.*, 2011, **83**, 1883-1889.
2. G. T. Walker, M. C. Little, J. G. Nadeau and D. D. Shank, *Proceedings of the National Academy of Sciences of the United States of America*, 1992, **89**, 392-396.
3. C. J. Kim, D. I. Lee, C. Kim, K. Lee, C. H. Lee and I. S. Ahn, *Anal. Chem.*, 2014, **86**, 3825-3833.
4. J. T. Liu, L. Zhang, J. P. Lei, H. Shen and H. X. Ju, *ACS Appl. Mater. Interfaces*, 2017, **9**, 2150-2158.
5. L. Z. Swisher, A. M. Prior, M. J. Gunaratna, S. Shishido, F. Madiyar, T. A. Nguyen, D. H. Hua and J. Li, *Nanomed.-Nanotechnol. Biol. Med.*, 2015, **11**, 1695-1704.
6. J. W. Tian, L. Ding, Q. B. Wang, Y. P. Hu, L. Jia, J. S. Yu and H. X. Ju, *Anal. Chem.*, 2015, **87**, 3841-3848.
7. S. Fuchs, H. Otto, S. Jehle, P. Henklein and A. D. Schluter, *Chem. Commun.*, 2005, DOI: 10.1039/b415651j, 1830-1832.
8. Y. Song, H. F. Fan, M. J. Anderson, J. G. Wright, D. H. Hua, J. Koehne, M. Meyyappan and J. Li, *Anal. Chem.*, 2019, **91**, 3971-3979.